Experimental characterisation of different hermetically sealed horizontal, cylindrical double vessel Integrated Collector Storage Solar Water Heating (ICSSWH) prototypes

Mervyn Smyth[a],*, Jayanta Deb Mondol[a], Ronald Muhumuza[a], Adrian Pugsley[a], Aggelos Zacharopoulos[a], Dominic McLarnon[b], Cesare Forzano[c], Annamaria Buonomano[d], Adolfo Palombo[d],

[a] Centre for Sustainable Technologies (CST), School of Architecture and the Built Environment, Ulster University, Newtownabbey, Northern Ireland, UK
[b] SolaForm Ltd, Block 26, IUL, BT37 0QB, Northern Ireland, UK
[c] Faculty of Science and Technology, Free University of Bozen-Bolzano, Bozen-Bolzano, Italy
[d] Department of Industrial Engineering, University of Naples Federico II, Naples, Italy

ABSTRACT

Existing Integrated Collector Storage Solar Water Heaters (ICSSWHs) are typically simple and low-cost devices that combine heat collection and storage functions in one unified vessel. However, during non-collection periods they are affected by higher heat loss characteristics when compared to standard solar collector systems. This paper introduces the design evolution of new horizontal cylindrical ICSSWH prototypes developed at Ulster University that use novel, patented double vessel, thermal diode features (to enhance heat retention during non-collection periods) achieved by incorporating a liquid-vapour phase change material (PCM) with a very low pressure annular cavity. The energy performance evaluation and characterisation of different prototype designs under solar simulated experimental conditions has been conducted and the subsequent parametric analysis presented. A balance between performance and physical/operational considerations is necessary to ensure that new and practical design solutions (in materials, fabrication and assembly) can be formulated to improve the performance of the ICSSWHs within the limits of commercial reality. The importance of augmenting heat transfer across the annulus cavity has been demonstrated with improvement of the cold-start daily collection efficiency from around (η_{col}) of 20% (no HTF), to >55% when the annulus is evacuated to remove non-condensable gases and form a liquid-vapour phase change thermal diode. Annulus thermal diode heat transfer coefficients of around (U_{fr}) 35 W/m^{2}K in forward mode and 2 W/m^{2}K in reverse mode have been demonstrated. Diurnal thermal efficiencies ($\eta_{col\ 24}$) of 22% have been measured, but values of 39% have been identified as achievable in the longer-term development of presented ICSSWH.

KEYWORDS

Solar thermal collector, ICSSWH, double vessel, thermal diode, solar simulator

1.0 INTRODUCTION

Integrated Collector Storage Solar Water Heaters (ICSSWH) are simple, low cost solar devices. The original ICSSWH systems consisted of exposed blackened tanks of water left out to heat in the sun. Used on a few farms and ranches in the South-West USA in the late 1800s, they were reportedly capable of producing water hot enough for showering by the late afternoon on clear days [Butti and Perlin, 1981]. ICSSWHs have developed significantly since these early units and their potential to broaden the scope of current small-scale solar hot water systems for single and multi-family dwellings, particularly in warm climates is apparent. Their continual development and improvement as simple, reliable and low cost configurations is essential to achieve increased interest in the general solar heat market globally.

The development of ICSSWH systems is detailed in Smyth et al. [2006] and more recently by Singh et al. [2016], along with their tendency to suffer significant ambient heat loss, especially at night-time and during non-collection periods. Many recent studies have focused on the improvement of the thermal performance of ICSSWH systems through the development of the thermal diode ICSSWH (based on De Beijer's [1998] double vessel concept) using liquid to vapour phase change. The use of liquid/vapour phase change materials in solar thermal technologies is not new, the heat pipe principle is recognised as one of the most efficient passive heat transfer technologies available. Jouhara et al [2017] provide a comprehensive review on heat pipe technology and Shafieian et al [2018] presents the latest developments, progress and application of heat pipe as solar collectors. The use of liquid to vapour phase change with storage (a quasi-heat pipe with storage) was first applied in De Beijer's [1998] ICSSWH. Quinlan [2010] sets out the principle for a vertical cylindrical unit, using the same double vessel design first reported by De Beijer. This work and follow up investigations by Smyth et al. [2017a,b; 2018] detail the performance of prototype systems determined using experimental evaluation and dynamic simulation modelling. These studies created enhancements and optimisation of the design which led to the development of a pre-commercial, pre-heat ICSSWH known as the SolaCatcher [SolaForm, 2014]. The energy performance of another laboratory prototype, using innovative end cap arrangements, was investigated under different boundary and working conditions, using a suitably dynamic simulation model developed and implemented in a computer code written in MatLab environment. The model was been validated by experimental data gathered from testing carried out under the solar simulator facility at Ulster University. [Smyth et al 2019a; 2020].

Some work has looked at augmentation of the double vessel, thermal diode concept with external reflectors. Souliotis et al. [2011; 2017] optically analysed (through ray tracing) and experimentally studied a thermal diode ICS vessel design mounted horizontally inside a stationary truncated asymmetric compound parabolic concentrating (CPC) reflector trough. Muhumuza et al [2019a,b, 2020] report on the use of a novel ICSSWH mounted within an asymmetric formed reflector that was specifically designed to the ICS tank requirements, giving rise to the Asymmetric Formed Reflector with Integrated Collector and Storage (AFRICaS) system.

Several authors have experimented with the design format and have investigated different double vessel, thermal diode configurations, other than cylindrical. Cylindrical vessels offer significant advantages in structural integrity, material and fabrication time, but suffer prominent features that don’t lend themselves to easy building integration and aesthetic appeal. Kalogirou et al [2017] have published a comprehensive handbook that reviews the design and application of Building Integrated Solar Thermal Systems (BISTS). In their guide, they specifically report upon flat collector profiles and detail a flat double vessel, thermal diode concept developed by Smyth et al [2017a,b; 2019b]. The work reports upon the experimental performance characterisation of a Hybrid Photovoltaic/Solar Thermal Façade module compared to a flat Integrated Collector Storage Solar Water Heater module. Both units were modular and designed specifically to integrate into a vertical building façade. Lamnatou et al [2019] carried out a Life Cycle Analysis (LCA) of the unit and reported on issues related to human health, ecosystems and resources. Earlier work by Pugsley et al [2016] conducted a comprehensive evaluation on the experimental characterisation of a flat panel ICSSWH design that featured a PV absorber and a Planar Liquid-Vapour Thermal Diode (PLVTD). More recent work by Pugsley et al [2019] explores the principle of thermal diodicity and presents pioneering work to experimentally measure the heat transfer characteristics of a 0.15 m^2 passive Planar Liquid-Vapour Thermal Diode (PLVTD). The flexibility of the double vessel concept was demonstrated by Mondol et al [2013] where it was used in a solar augmented anaerobic digester design for small-scale biogas production. The lag in collection and improved thermal retention created a more stable inner vessel (digestor) temperature, minimising operational temperature fluctuations.

The work presented in this paper details the design evolution of horizontal ICSSWH prototypes developed at the Centre for Sustainable Technologies (CST) at Ulster University that use the novel, patented (a solar water heater, 2010) double vessel, thermal diode feature (to enhance heat retention during non-collection periods) achieved by incorporating a liquid-vapour phase change material (PCM) and very low annulus cavity pressures. The energy performance evaluation and characterisation of different prototype designs under solar simulated experimental conditions has been conducted and the subsequent parametric analysis has created improvements and optimisation that are instrumental in informing the development of a commercial ready design for deployment in the developing world.

2.0 THERMAL DIODE DESCRIPTION

A solar thermal diode is a mechanical technique that enables rapid heat collection of incident solar radiation on the absorber combined with thermal insulation of the collected heat in a storage tank to minimise heat loss during the night and non-collecting periods. A small volume of PCM (heat transfer fluid, HTF) resides in the low pressure annulus of two concentric cylindrical vessels and determines the forward and backward operational behaviour of the thermal diode as illustrated in Figure 1.

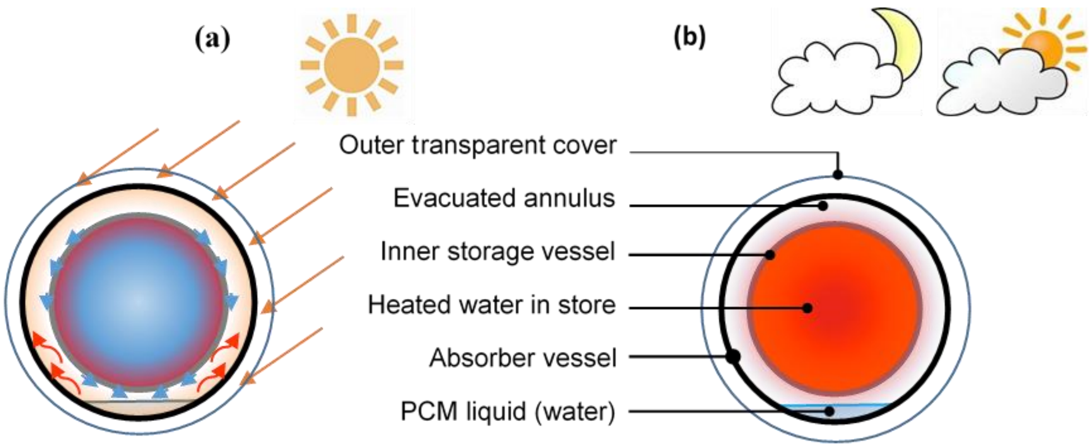

Figure 1: Operating principle of the ICSSWH design concept: (a) forward operation during thermal energy collection for a sunny period, (b) reverse operation during night-time and non-collecting periods [Muhumuza et al, 2019b]

In the forward mode, radiant solar heat evaporates the PCM HTF under partial vacuum in the annulus, which then condenses on the outer surface of the storage tank thereby releasing its latent heat of vaporisation to the store before returning to the sump. In the reverse operation mode, the 'partial' vacuum in the annulus (along with outer transparent cover) minimises convective and radiative losses to ambient. The presence of non-condensable gases in the thermal diode cavity (as indicated by the cavity pressure at a low temperature) significantly impairs the forward mode heat transfer rate [Boreyko et al, 2011; 2013]. Evacuating the cavity to the lowest total pressure possible, enables effective forward mode heat transfer. Vertical installations are preferred for achieving thermal stratification in the storage tank, which is often a requirement for cold/temperate climate conditions. However, horizontally mounted units could be just as good when operating in regions with significant solar resources. Figure 2 demonstrates one of the horizontally mounted prototypes - the 'SolaCatcher' installed (and combined with an integrated PV panel) and operated in Northern Botswana.

Figure 2: Installed horizontal 'SolaCatcher' prototype in Northern Botswana

The aim of the work presented in this study is to deliver an optimised blueprint for the ICS thermal diode design, that has a relatively good (comparative) performance but presents a much simpler design in materials and components, needs no parasitic pumping or control power to operate, is easy to install and connect and offers the potential for much lower costs and therefore more cost-effective hot water for many in the developing world. The metal/metal evacuated concept makes a much more robust unit, which makes them less susceptible to environmental physical damage than existing commercial glass/metal evacuated ICSSWHs. Furthermore, from a manufacturing perspective, the metal/metal vessel concept doesn't need specialised fabrication/assembly equipment or facilities but can be produced in traditional metalworking facilities already experienced in making water storage tanks.

3.0 THE DOUBLE VESSEL, THERMAL DIODE ICSSWH

The unit presented in Figure 2 represents years of developmental work conducted in the Ulster University CST laboratories. Many different variants have been realised and tested as part of the evolutionary progression leading to the current design. All have utilised the thermal diode operating principle combined with a horizontal cylindrical tank-in-tank configuration, similar vessel dimensions and tubular stainless-steel vessel materials. Each vessel was coated with a matt black film of black stove paint, enclosed within a cylindrical transparent aperture cover and mounted on a frame that permitted the inclusion of an external reflector and inlet/outlet ports. This paper compares and contrasts the results obtained from experimental tests on design variants, examining the influence of different operating parameters (pressure, heat transfer fluid, irradiation), and the effect of various design options concerning insulation, heat exchanger integration and vessel end sealing mechanisms.

The main variable design features used to delineate the concept classification and investigation was the vessel end sealing mechanism; either hermetic polymer end cap or metal weld. Figure 3 depicts the various units evaluated. The main geometrical and thermal features of the ICSSWH prototypes presented are detailed in Table 1.

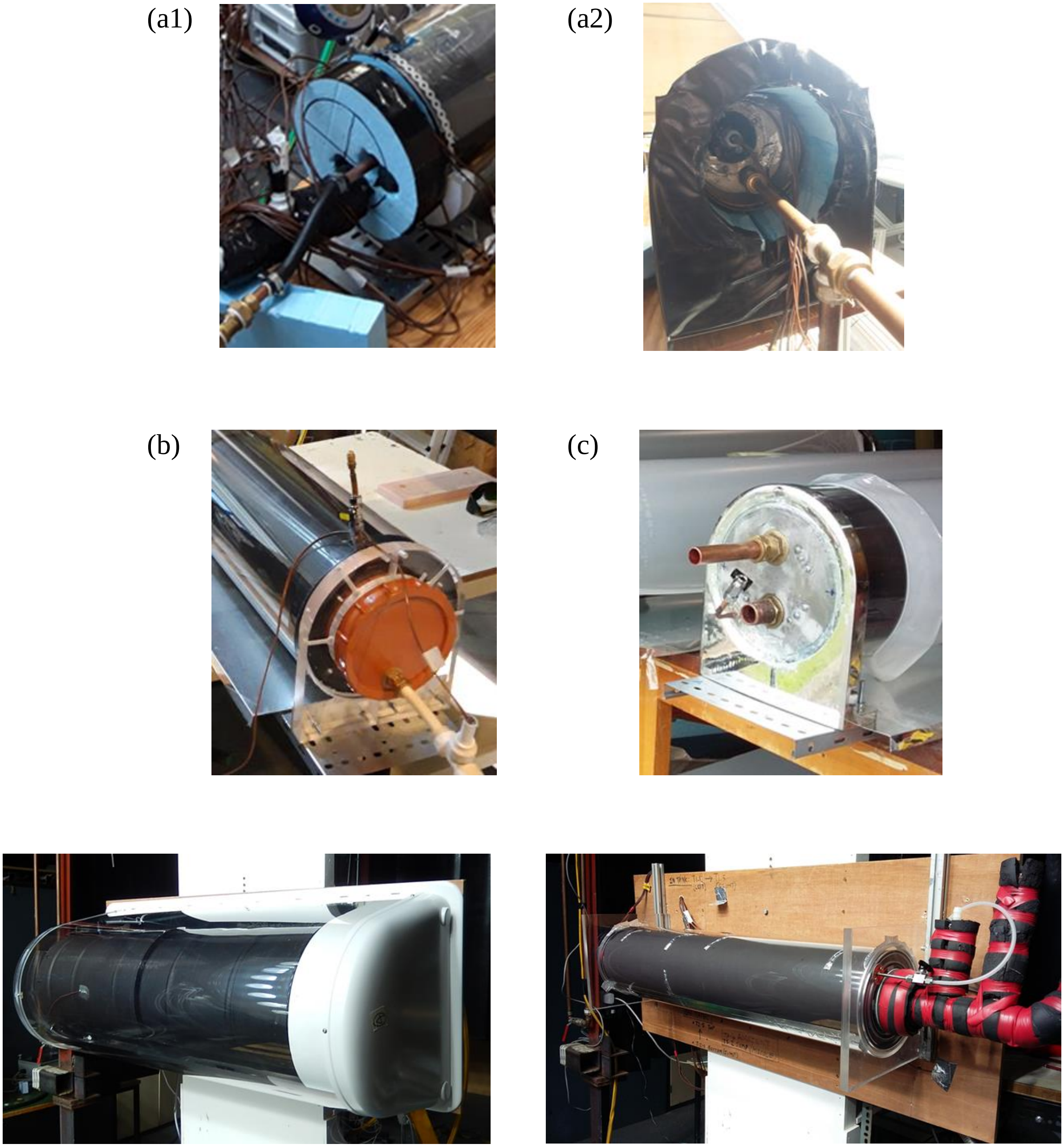

(a1) (a2) (b) (c) (d) (e)

Figure 3: Different horizontal double vessel, thermal diode ICSSWH prototypes investigated in the present study

Table 1: Investigated ICSSWH prototype main features

	a1. seam welded cone	a2. inset seam welded cone	b. PVC cup insert	c. ABS hub with gasket	d. seam welded dish	e. Acrylic hub with gasket
Vessel (SS): Capacity, Length & Diameter	25.8 litres 1.43m 200mmØ	24.2 litres 1.41m 200mmØ	30.8 litres 1.62m 200mmØ	28.8 litres 1.63m 200mmØ	47.5 litres 1.11m 360mmØ	16.5 litres 1.01m 200mmØ
Volume-to-absorber area ratios	0.029 m^3/m^2	0.027 m^3/m^2	0.030 m^3/m^2	0.028 m^3/m^2	0.038 m^3/m^2	0.026 m^3/m^2
Transparent cover	PETG, single layer (scuffed)	PETG, single layer	PETG, single layer	PETG, single layer	PETG, double layer	Acrylic, single layer
Solar Source: Irradiance & angle from the horizontal	706Wm^2 15°	700Wm^2 45°	715Wm^2 90°	730Wm^2 0°	661Wm^2 90°	730Wm^2 45°
Back reflector	yes/no	yes/no	yes	yes	no	no
Wetting mechanism	Capillary matting (partial)	Capillary matting (partial)	Capillary matting (good fit)	Capillary matting (good fit)	Film spray	Capillary matting (good fit)

Unit (a) was a fully welded stainless steel, double vessel arrangement. There were 2 differing configurations; (a1) and (a2). Both variants were identical and utilised the same sloped end cone design to bring the inner and outer vessels together to enable a hermetic seam weld to be formed. The depth of the welded seam however differentiated the designs. Unit (a1) had a flush end weld whilst unit (a2) had an inset (by 100mm) end weld. Unit (d) was also a fully welded stainless steel, double vessel arrangement, but differed in its diameter and length and the type of wetting mechanism. Units (b), (c) and (e) comprised 2 concentric stainless steel tubes that were connected and thus hermetically sealed using a polymer end cap and gasket seal. Unit (b) utilised an inserted PVC cap with a removable lid. Units (c) and (e) utilised ABS and acrylic, respectively, with the 2 concentric stainless steel tubes inserted into recessed gasketed grooves to provide the hermetic seal. The majority of materials used (and therefore characteristics) for all the units were common. The transmittance-absorptance product ($\tau\alpha$) of the 1mm thick PETG transparent cover was 0.75 with a thermal conductivity of 0.25 W/mK. The 1.5mm thick stainless steel used to make the vessels had a thermal conductivity of 16 W/mK and the 5mm thick PVC end caps had a thermal conductivity of 0.18 W/mK. Acrylic and ABS both have a thermal conductivity of around 0.2 W/mK.

Pugsley et al [2020a] presents a collective review of the importance of the volume-to-absorber area ratios (V/A_{ab}) in ICSSWH design. Smyth et al. [2006] and Singh et al. [2016] presents numerous studies on ICSSWH vessel design, including single or multiple cylindrical, cuboid, triangular, trapezoidal and pyramid tanks. Volume-to-absorber area ratios range from 0.05 to 0.3 m^3/m^2 with 0.1 m^3/m^2 being a typical vessel size. Small volumes of stored water cause large diurnal temperature fluctuations in solar heating systems. Larger volumes reduce fluctuation magnitudes thereby reducing summertime overheating and wintertime freezing risks, but the resulting reduced maximum temperatures can increase legionella risks. Schmidt & Goetzberger [1990] suggest V/A_{ab}>0.07 m^3/m^2 for Northern European climates to reduce freeze risks. Amerongen et al. [2013] suggests limiting criteria of V/A_{ab} <0.03 m^3/m^2 and V/A_{ab} <0.06 m^3/m^2 for northern and southern European climates, respectively in respect of controlling legionella risk in direct-flow solar water heating systems. The designs examined in this study all have volume-to-absorber ratios in the range 0.025 < V/A_{ab} <0.04 m^3/m^2 and are primarily intended for use in sunny equatorial, tropical and sub-tropical regions. Choice of volume-to-absorber ratio is partly influenced by the need to minimise legionella risk, but also by the need to minimise unit weight and material costs without compromising structural integrity. Units with larger volume-to-absorber ratios inherently require much heavier gauge stainless steel together with structural reinforcements to prevent implosion associated with partial vacuum annulus cavity pressures.

4.0 EXPERIMENTAL SETUP DESCRIPTION

The horizontal SolaCatcher prototypes (typical setup shown in Figure 4) were experimentally evaluated using the state-of-the-art indoor Solar Simulator facility at the Centre for Sustainable Technologies (CST), Ulster University [Zacharopoulos, 2009]. The indoor solar simulator testing facility consists of 35 high power metal halide lamps arranged in 7 rows of 5 lamps. Each lamp is equipped with a rotational symmetrical paraboloidal reflector that provides a light beam of high collimation. In order to achieve uniform distribution of light intensity on the test area, a lens is inserted into each lamp to widen the illumination of light. The combination of reflector-characteristics, lens and lamps ensures a realistic simulation of the beam path, spectrum and uniformity. The solar simulator control panel maintained the constant level light intensity automatically on the collector surface via a pyranometer mounted at the centre of the test plane. Testing via Solar Simulator adhered to standard ISO 9806:2017 regarding the use of a Solar Simulator and instrumentation, including, irradiance, uniformity, collimation, spectral distribution and IR thermal radiation. Indoor solar thermal simulator testing provided consistent/repeatable test conditions as well as instantaneous and average collection efficiencies. Heat loss coefficients and heat retention efficiencies are achieved from overnight cool-down period testing.

T-type Copper/Constantan Thermocouples with ±0.5 K accuracy measured the temperatures in the water, on vessel surfaces, and ambient air temperatures. All thermocouples were fabricated in-house, calibrated and mounted onto and within the prototype units to ensure accurate temperature representation. Under the solar simulator, the lamps illuminated the test rig at various incidence angles to the horizontally mounted ICSSWH as shown in Figure 4. The irradiance value was measured for each test. The intensity varied between 660 and 730±10 Wm^2 on the transparent cover which is typical of the mean hourly global horizontal solar radiation during the period of 6 hours representing a typical period of utilisable solar energy between 10:00 a.m. to 4:00 p.m. for most equatorial locations [Weather Data, 2019]. A calibrated pyranometer (Kipp & Zonen-CM4) of sensitivity 6.87$\mu VW/m^2$ was used to measure incident simulated radiation levels on each ICSSWH. A digital pressure gauge (Druck DPI104-1) with 0.05% full-scale accuracy measured annulus cavity pressure. The acquisition of experimental measurements was done under no draw-off conditions for a total period of 24 hours comprised of 6 to 8 hours of solar thermal collection and 16 to 18 hours of cool-down (heat retention). All sensors were linked back to dedicated channels of a data logger (Delta-T DL2e), which sampled every 5 s and recorded average temperatures on 5-min intervals.

The presented ICS prototype units (as non-separable solar collectors) have been tested using an adapted version of ISO 9459-4 (British Standards Institution, 2013) based on heat loss tests and warm-up tests. The testing and characterisation of ICSSWH concepts has long been a point of discussion for researchers. Tripanagnostopoulos et al (2002) developed a method that has been used by many authors since. The method used was considered simpler to other methods presented by Aranovitch et al (1986) and Faiman (1984), regarding the comparison of tests relating to different

ICS systems, using the water temperature in the system (ICS) tank from bottom to top. This current work uses Tripanagnostopoulos et al's (2002) quasi-steady state method to present the thermal performance and characterisation of the concept prototypes. This does not directly yield performance criteria to certified standards, but rather permits the direct comparison of the prototypes being developed, towards future work in commercialisation and solar Keymark accreditation. The adapted ISO 9459-4 test standard is used to give guidance and quality assurance in instrumentation and facility set up. Previous work [Smyth et al, 2017; Muhumuza et al, 2019a,b, 2020] regarding the thermal performance characterisation of ICSSWHs details the test procedures of ICS characterisation under indoor solar simulated conditions.

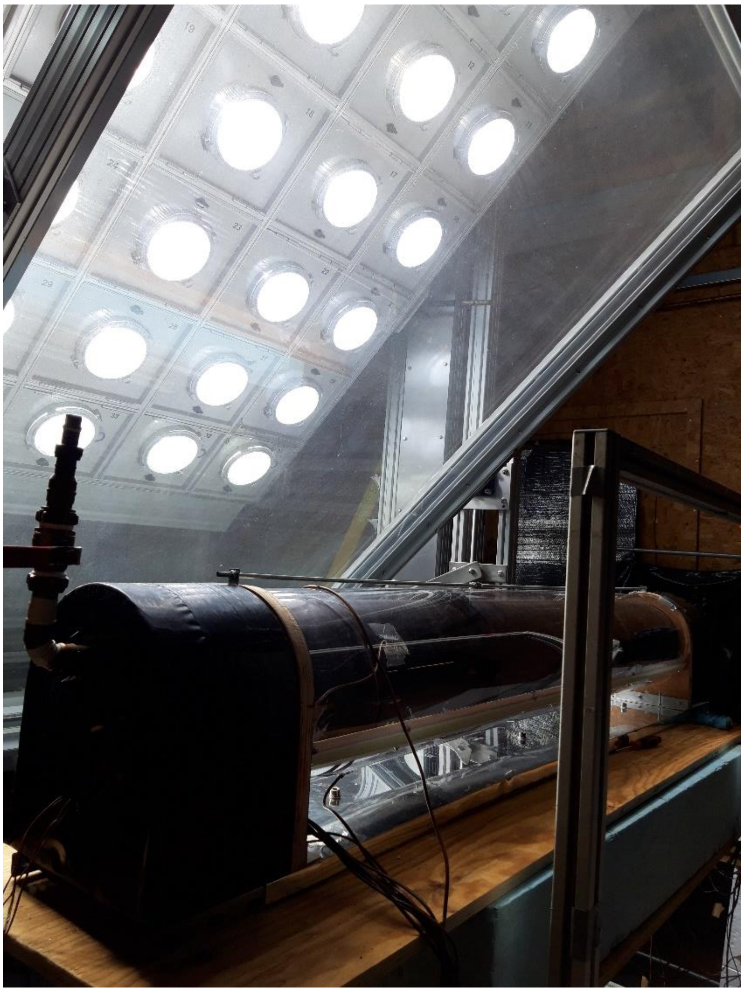

Figure 4: Typical experimental set up for a prototype under the solar simulator

5.0 EXPERIMENTAL RESULTS AND DISCUSSION

A series of experimental investigations were conducted to determine the performance of the different units under differing incident angles and levels of irradiance, varying storage capacities, with and without insulation, with and without a planar reflector, various transparent cover(s) arrangements, and applying different annulus pressures. Over 60 indoor solar thermal simulator tests were conducted, spanning a 4 year period of component and unit design development.

Performance characterisation consisted of evaluation of temperature profiles, the mean 6 hour collection efficiency and nominal solar heating efficiency curves, the mean 12 and 18 hour heat retention efficiency and thermal loss coefficients, the overall thermal transmission in forward (f) heat transfer mode and reverse (r) insulation mode and the diurnal 24 hour thermal efficiency. Definitions of these parameters are given by Pugsley et al. [2020a] and have not been repeated here for the sake of brevity. This paper presents a condensed representation of the important findings observed over the extended period of investigation.

Temperature profiling

Figure 5 details the location of thermocouples and a typical vessel cross section with corresponding sensor temperature annotation: T_1 – average outer transparent surface temperature, T_2 - average outer (absorber/evaporator) vessel surface temperature, T_3 - average inner (storage/condenser) vessel surface temperature, T_4 – average water store temperature and T_{amb} - local ambient temperature. Other sensor annotation (not included) are HTF sump temperature at the base of the outer vessel and end cap temperatures.

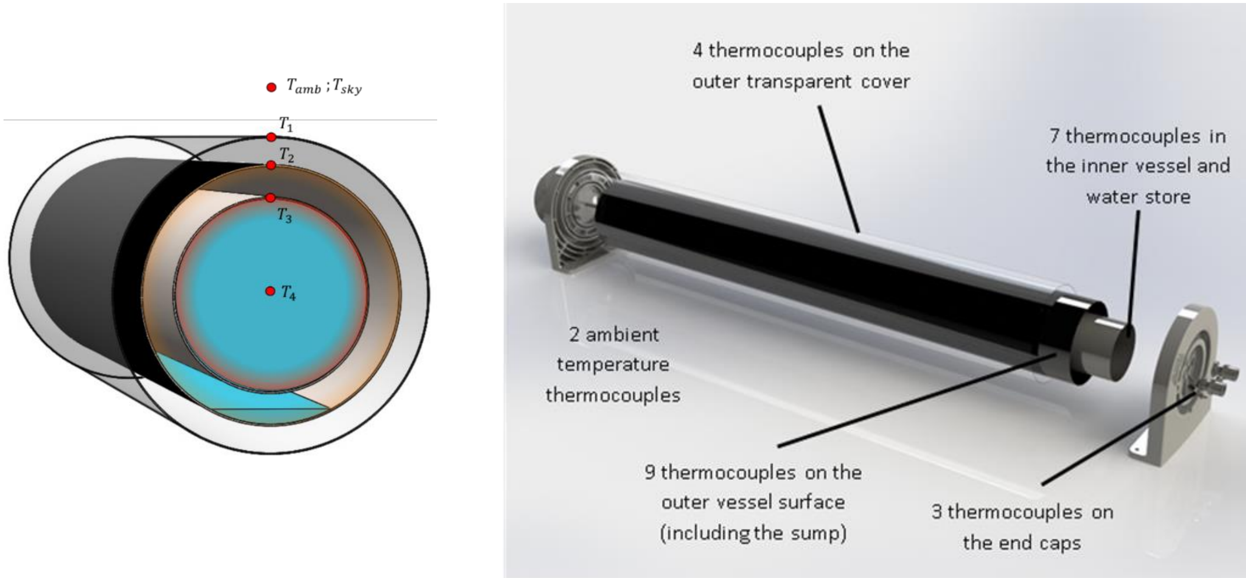

Figure 5. Typical cross section detail with corresponding sensor temperature annotation (left) and number of thermocouple located on ICS prototypes

Figures 6 to 10 detail the recorded temperature profiles for elements within various units, showing average outer and inner cylinder surface temperatures, HTF sump, average water store temperature and local ambient temperature. Figure 6 shows the temperature plots for components in the base line unit a1. Figures 7 to 9 shows the temperature plots for components in unit a2.; base line, without reflector and without vacuum and reflector. Figure 10 shows the temperature plots for components in the base line unit c.

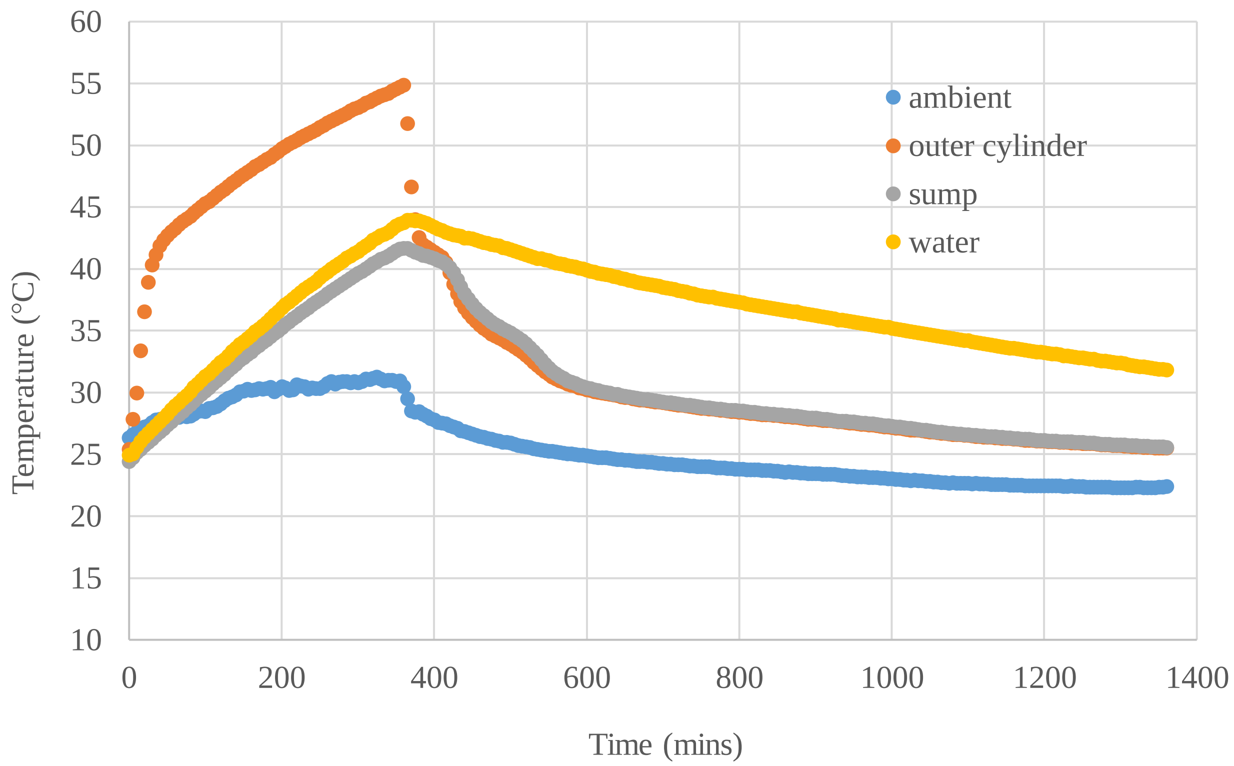

Figure 6. Measured temperature plots for components in the base line unit a1. (under 706 ±10 W/m^2 solar simulated radiation during the 6 hour collection period)

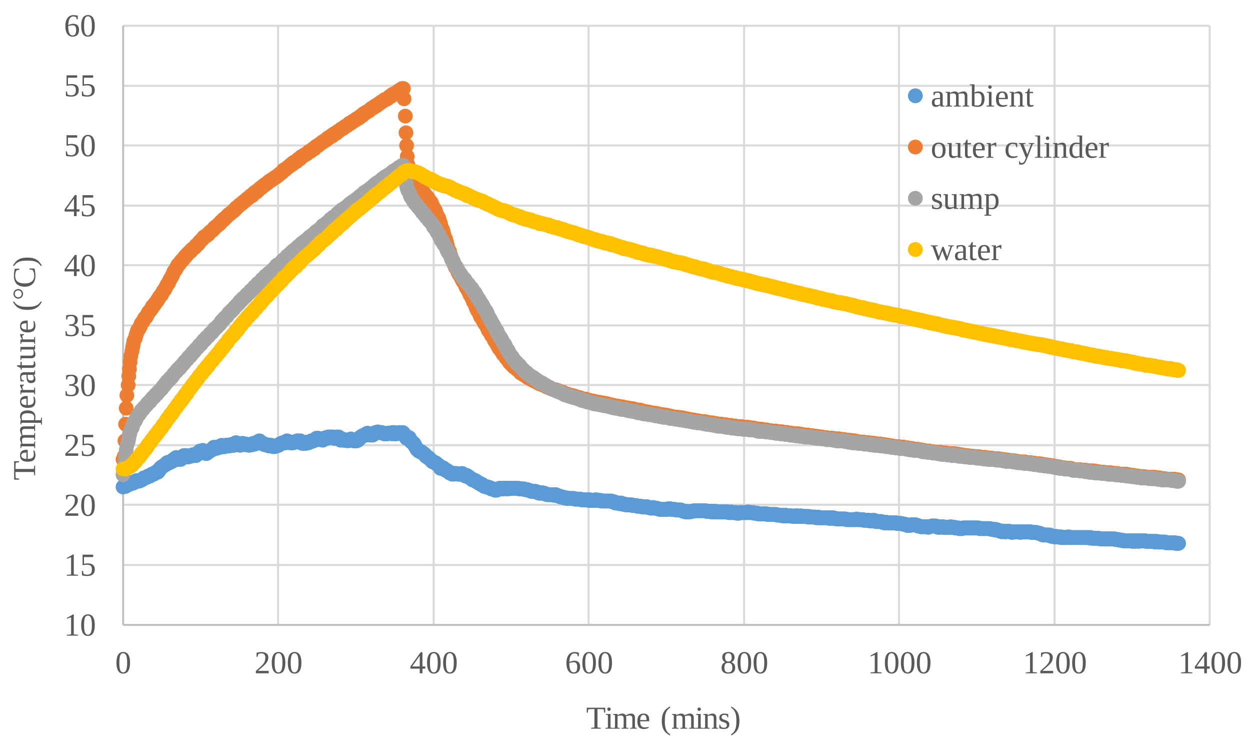

Figure 7. Measured temperature plots for components in the base line unit a2. (under 700 ±10 W/m^2 solar simulated radiation during the 6 hour collection period)

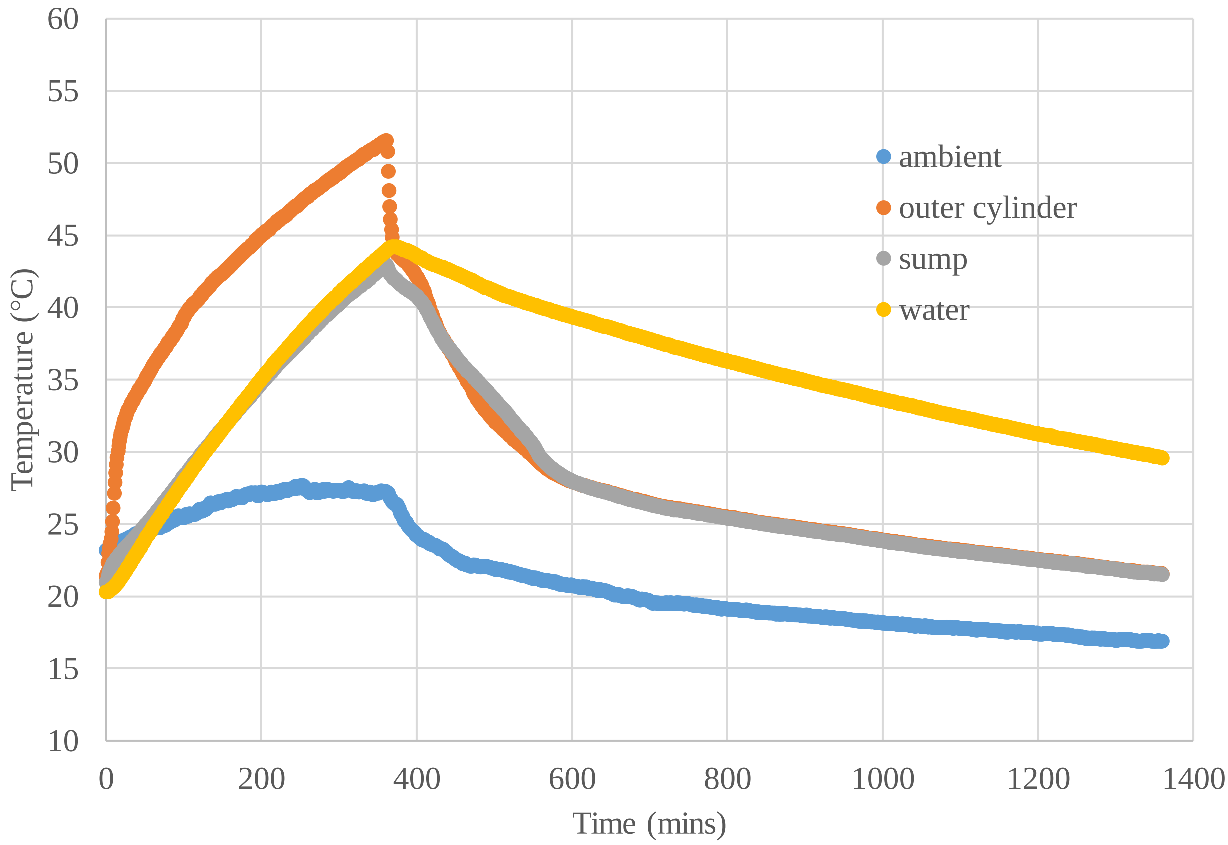

Figure 8. Measured temperature plots for components in unit a2. with no reflector (under 694 ±10 W/m^2 solar simulated radiation during the 6 hour collection period)

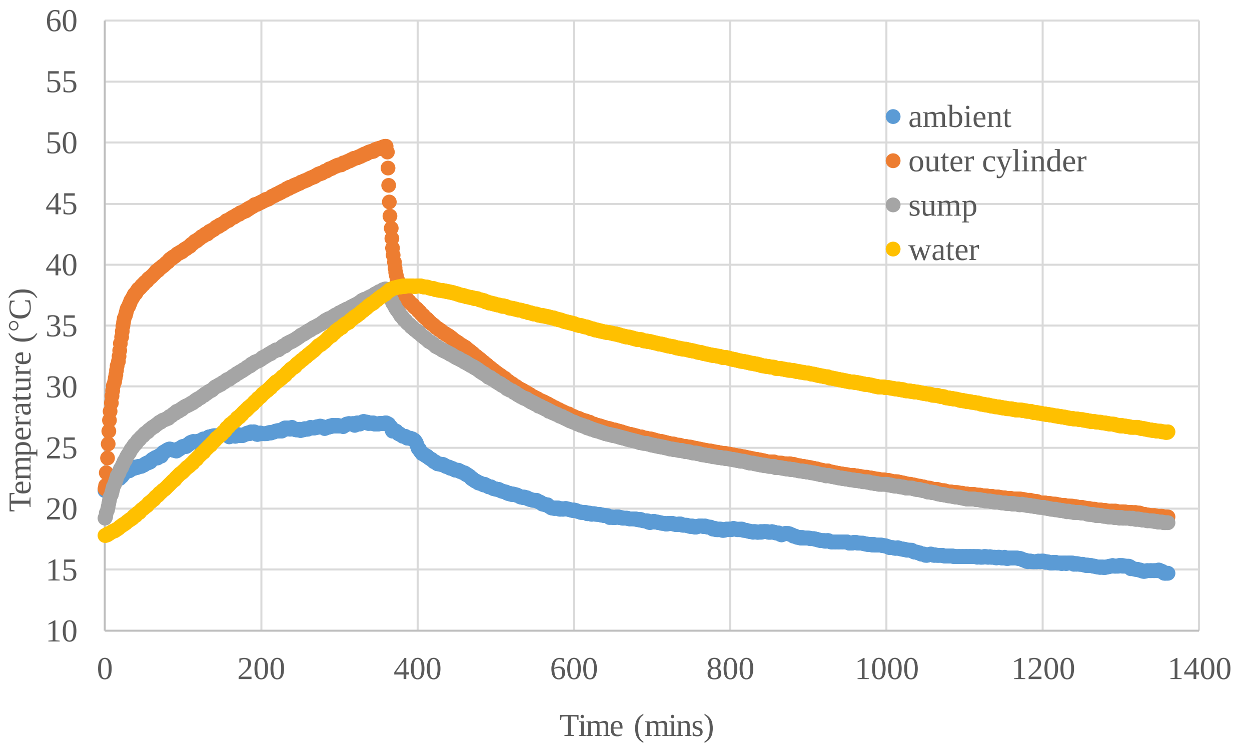

Figure 9. Measured temperature plots for components in unit a2. with no vacuum and no reflector (under 696 ±10 W/m^2 solar simulated radiation during the 6 hour collection period)

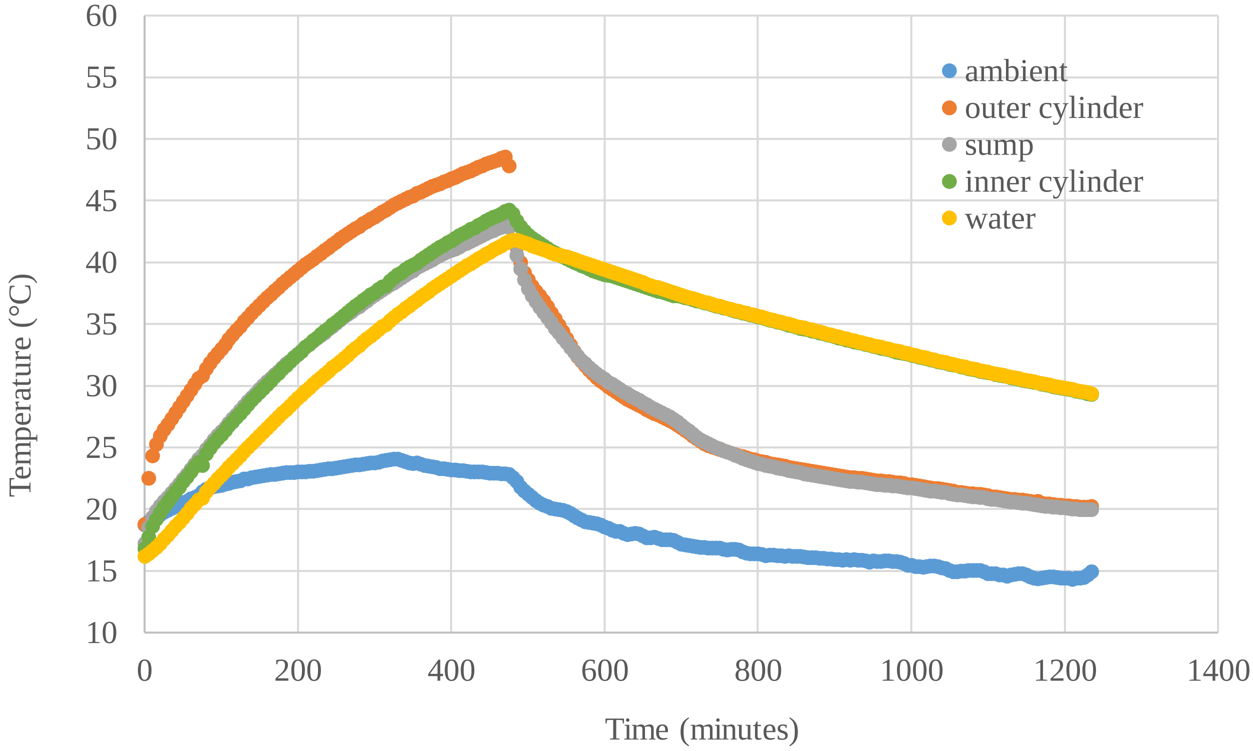

Figure 10. Measured temperature plots for components in the base line unit c. (under 715 ±10 W/m^2 solar simulated radiation during the 6 hour collection period)

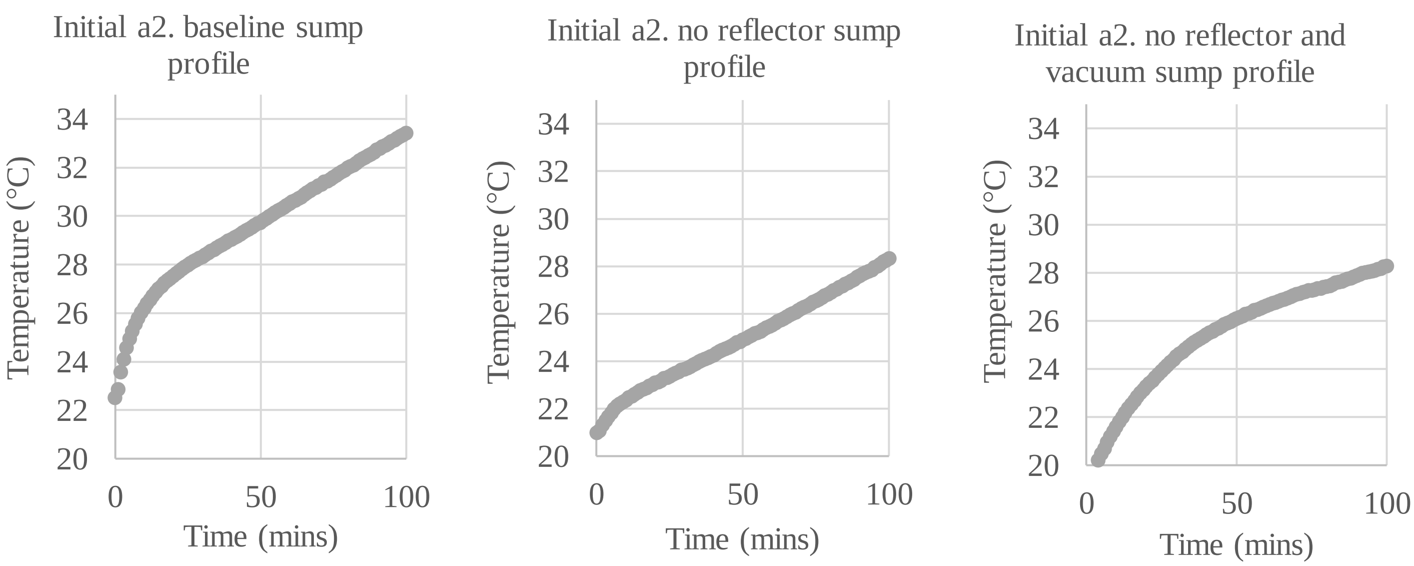

Figure 11. Initial sump temperature plots for a2 units (baseline - left; no reflector - middle; no reflector and no vacuum - right) from figures 7, 8 and 9

All the measured temperature plots (Figures 6 to 10) in each horizontal, double vessel, thermal diode unit (including those not shown) exhibit the same standard profile pattern and differentiation. During the collection phase, there is an initial rapid rise in the (average) outer absorbing cylinder temperature, followed by a gentler rise in the sump, inner cylinder and water temperatures.

Figures 7 to 9 illustrates the various plots for different unit a2 configurations and figure 11 shows the initial sump temperature plots for the 3 units in detail; baseline unit (with reflector and vacuum), unit without reflector and unit without vacuum and reflector, extracted from figures 7, 8 and 9. The impact of different (or rather lack off) component elements can be observed in figure 11 through the differing sump temperature profiles. The removal of the planar reflector at the base of the outer absorbing vessel, just below the HTF sump, results a similar sump and water temperature. As there is no reflected solar radiation incident on base of the absorber vessel, the sump temperature does not initially rise rapidly (exhibiting an almost linear like rise) which results in a slower HTF evaporation rate, borne out by the lower collection performances highlighted later in the analysis. Likewise, the lack of vacuum also shows a difference in sump and water temperatures. Due to the absence of the thermal diode evaporation/condensation heat transfer mechanism, heat transfer to the inner vessel is curtailed and so the water temperature rises at a much slower rate, again borne out by lower collection performances. During the cool-down phase, the outer vessel surface temperatures rapidly drop away towards ambient, but never converge due to radiative heat loss from the inner vessel/water maintaining the surface temperature above ambient.

Collection performance

The mean collection efficiency η_{col} of the various units over the testing period is given by the ratio of the amount of thermal energy collected Q_{col} to the total energy incident on the aperture Q_{ap} and is shown in Equation 1.

$$\eta_{\mathrm{col}} = Q_{\mathrm{col}}/Q_{\mathrm{ap}} = \left[\mathrm{m_w} C_{\mathrm{p,w}}\left(T_{\mathrm{w,f}} - T_{\mathrm{w,i}}\right)\right] / \left(I_{\mathrm{avg}} A_{\mathrm{ap}} \Delta t\right) \quad (1)$$

where Δt is the collection period (seconds) under the solar simulator, A_{ap} is the collector area (m^2) and I_{avg} is the constant average light intensity ($\mathrm{W/m^2}$) as measured by the pyranometer, $\mathrm{m_w} = \rho V_T$ is the mass of water in the inner storage vessel (kg), ρ is the water density ($\mathrm{kg/m^3}$), V_T is the inner vessel storage volume (m^3), $C_{\mathrm{p,w}}$ is the specific heat capacity of water at constant pressure ($\mathrm{J\,kg^{-1}K^{-1}}$) and $T_{\mathrm{w,i}}$ and $T_{\mathrm{w,f}}$ (°C) are the average initial and average final temperature of the stored water. T_{w} and T_{a} are the average water temperature and average ambient air temperature (°C), respectively.

Table 2: Collection characteristics for the investigated ICSSWH prototypes

	Test	Annulus pressure	Irradiation ($\mathrm{Wm^2}$)	Planar reflector	Cold-start daily collection efficiency (6hrs) (η_{col})
a1. seam welded cone	No HTF	-952 mb	615	yes	0.27
	Low intensity	-952 mb	615	yes	0.42
	Base case	-951 mb	706	yes	0.47
	No reflector	-953 mb	609	no	0.38
a2. inset seam welded cone	No vacuum	0 mb	692	yes	0.53

	Base case	-955 mb	700	yes	0.57
	No reflector	-943 mb	694	no	0.55
	No vacuum No reflector	0 mb	696	no	0.50
b. PVC cup insert	Base case	-986 mb	715	yes	0.54
c. ABS hub with gasket	Insulated end caps	-980 mb	731	yes	0.61
d. seam welded dish	No HTF film Double cover	-955 mb	661	yes	0.19
	Base case HTF film Double cover	-955 mb	661	yes	0.52
	Vertical HTF film Double cover	-950 mb	694	yes	0.52
e. Acrylic hub with gasket	Base case	-950 mb	730	no	0.61

Table 2 details the test set parameters and the 6 hour "cold-start" daily collection efficiency (η_{col}) for a range of investigated ICSSWH prototypes where all tests were initiated under similar conditions of testing procedure, exposure to radiation and ambient temperature (±2°C from the vessel water temperature). It is clear that some physical elements are key to the operational performance. The absence of a HTF makes a very big difference to the collection efficiency (η_{col}), reducing collection by almost half when it is omitted. Removing the reflector reduces η_{col} by between 2 and 9% and the lack of vacuum reduces η_{col} by about 5% in the cases tested. Good insulation on the end caps is also a factor. Units b, c and e had insulation on the polymer end caps, but unit c, had slightly less insulation (and greater surface area projection due to its construction) and exhibited 6% less collection. The lack of end cap insulation is more apparent on performance during the cooldown phase.

The thermal output of ICSSWH systems is illustrated according to Tripanagnostopoulos et al (2002) in the form of nominal solar heating efficiency curves where the x-axis is the solar thermal condition ($(T_w\text{-}T_a))/I_{ave}$) and the y-axis is the instantaneous solar thermal collection efficiency (η_T). On such plots, the y-axis intercept indicates maximum solar thermal efficiency under zero heat loss conditions ($\eta_T = F \times \tau \times \alpha$ where $T_w - T_a = 0$); the line gradient ($F \times U_L$) represents the overall heat loss coefficient referenced to the absorber area (A_{ab}); and the x-axis intercept indicates the stagnation condition. In traditional collectors (flat plate, etc), the y-axis intercept usually gives the collector optical efficiency (η_{col}) as there is near perfect absorber-to-fluid heat transfer under these conditions (Heat removal factor, $F>0.95$) and the overall efficiency is determined by the transmission absorption product ($\tau\alpha$). However, in previous thermal diode studies, the heat removal factor has been observed to be $F<0.95$ due to the resistance of the thermal diode.

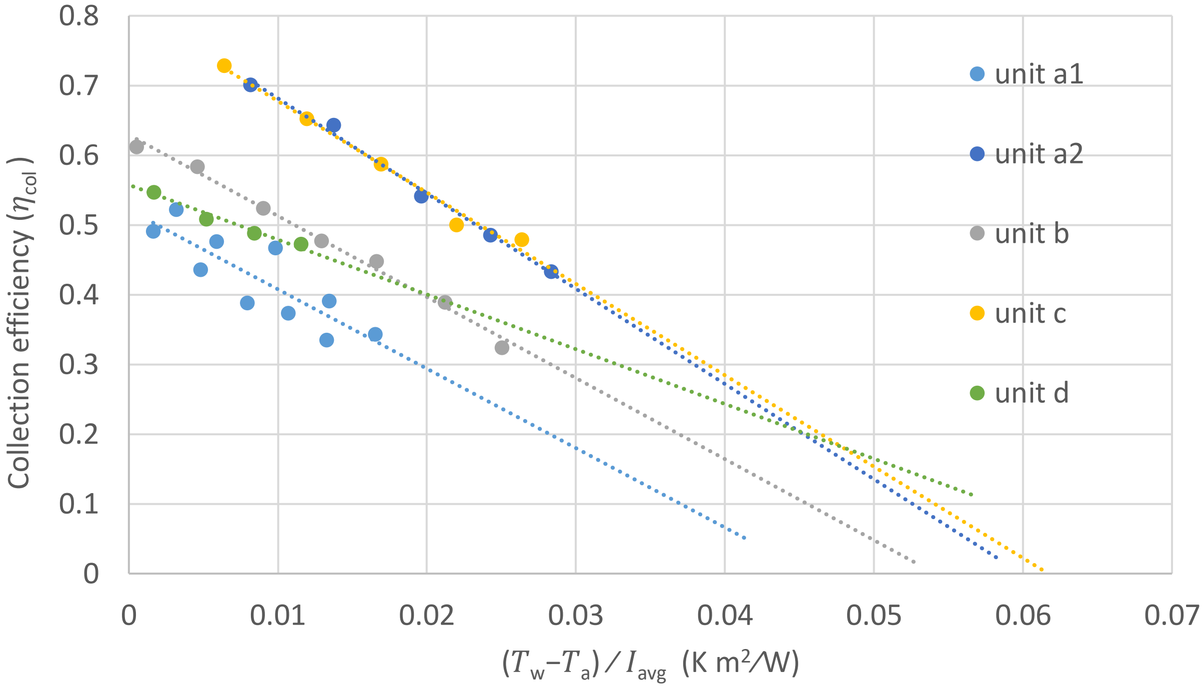

Figure 12. Nominal solar heating efficiency for various double vessel ICSSWHs (under constant solar simulated radiation during the 6 hour collection period)

Table 3: Collection characteristics for the ICSSWH prototypes shown in Figure 12

	Test variant	Cold-start daily collection efficiency (6hrs) (η_{col})	$F(\tau\alpha)$	($F \times U_L$)	Operational collection efficiency ($\eta_{col(0.035)}$ at $(T_w\text{-}T_a)/I_{ave}$ = 0.035m^{2}K/W
a1. seam welded cone	Base case	0.47	0.52	-11.39	0.12
a2. inset seam welded cone	Base case	0.57	0.82	-13.66	0.34
b. PVC cup insert	Base case	0.54	0.63	-11.63	0.22
c. ABS hub with gasket	Base case	0.61	0.81	-13.11	0.35
d. seam welded dish	Base case with HTF film Double cover	0.52	0.56	-7.86	0.28

Figure 12 and Table 3 detail the 'simple' linear nominal solar heating efficiency plots and corresponding mathematical characterisation for the 5 base case, double vessel ICSSWHs (under constant solar simulated radiation during the 6 hour collection period). Base case relates to units having HTF wetting the evaporator, annulus cavity being under vacuum pressure, and the prototype being fitted with a reflector, insulated end caps and a single transparent cover (as listed in Tables 1 and 2) for that test series. Amongst the performance metrics used in Table 3 are the "cold-start" daily collection efficiency and the "operational" collection efficiency. The former describes the overall daily collection efficiency when the test is commenced with a stored water temperature equal to the ambient temperature. The latter is intended to be representative of a notional typical operating condition $(T_w\text{-}T_a) / I_{ave}) \approx 0.035 m^2K/W$ as proposed by Pugsley et al. [2020a] who established a benchmark target of $\eta_{col} \approx 60\%$ representing a performance broadly comparable to basic conventional solar thermal collectors.

Unit a2. inset seam welded cone and unit c. ABS hub with gasket, are observed to offer the best collection performance with cold-start daily collection efficiencies (η_{col}) of 57% and 61%, respectively. Similarly, their zero-loss performances ($F(\tau\alpha)$) are 82% and 80%, respectively. Both units (from a fabrication and assembly perspective) had superior materials and techniques and so the removal of cover 'scuffs', better application of matt black coatings, capillary mat contact and vessel bracing structures did in part lead to better $F(\tau\alpha)$ values. The improved mean collection efficiencies highlight the benefit of design enhancements to remove unnecessary end cap heat losses. This is explored later in the analysis. Unit d. seam welded dish, suffers from a lower $F(\tau\alpha)$, but benefits from a much shallower gradient ($F \times U_L$) indicating a much better capture of collected and converted heat. This is probably related to the better V/A_{ab} ratio due to the larger thermal store as well as superior heat transfer properties of the thermal diode. Unit d. had a V/A_{ab} ratio of $0.038 m^3/m^2$ and a falling film thermal diode whilst units a2. and c. had much lower V/A_{ab} ratio at around $0.028 m^3/m^2$ and featured passive thermal diodes based on capillary matting.

In terms of the operational collection efficiency at $(T_w\text{-}T_a) / I_{ave}) \approx 0.035 m^2K/W$, again, units a2. and c. exhibited the best performance at 34% and 35%, respectively. Unit d. with a low $F(\tau\alpha)$ but better ($F \times U_L$) is a closer competitor achieving 28%. Compared to the collection performance of other ICSSWHs, the current prototypes perform quite well. Pugsley et al [2020a] provides a comprehensive catalogue of key performance indicators for many ICSSWH research conducted around the world over the past 2 decades. The authors report that the minimum operational collection efficiency (η_{col} at $(T_w\text{-}T_a) / I_{ave}) \approx 0.035 m^2K/W$) reported in literature was 28%, the maximum was 59% and the average was 43%. Specifically compared to other double vessel, thermal diode systems, the performance of the presented units is reasonably good. A horizontal cylindrical tank-in-tank, selective coating, two-part CPC reflector, single glazed, insulated unit presented by Souliotis et al [2017] presents a mean collection efficiency of 31%. Muhumuza et al [2019b] report upon double vessel units with an aluminium outer vessel and a stainless steel outer vessel with cold-start daily collection efficiencies (η_{col}) of 47.4% and 51.6%, respectively. Pugsley et al [2020a] translates the performance to operational collection efficiencies of 28% and 31%, respectively. Follow on work by Muhumuza [2020] for their Asymmetric Formed Reflector with Integrated Collector and Storage (AFRICaS) system, states zero-loss performance of 48.5% and an operational efficiency of around 37%. The zero-loss performances of the single covered BIPV-PLVTD-ICSSWH collector in Pugsley et al [2020b] is 60% and their measured performances at the benchmark solar thermal condition (0.035 m^2K/W) is 49%.

Figure 13 compares the collector characterisation for unit a2. under different operating conditions to assess the impact of the vacuum, reflector and end insulation.

- Test 5 - unit a2. – atmospheric with HTF and reflector
- Test 6 - unit a2. – evacuated with HTF and reflector
- Test 8 - unit a2. – evacuated with HTF but no reflector
- Test 9 - unit a2. – evacuated with HTF, reflector but no end cap insulation
- Test 10 - unit a2. – atmospheric with HTF but no reflector

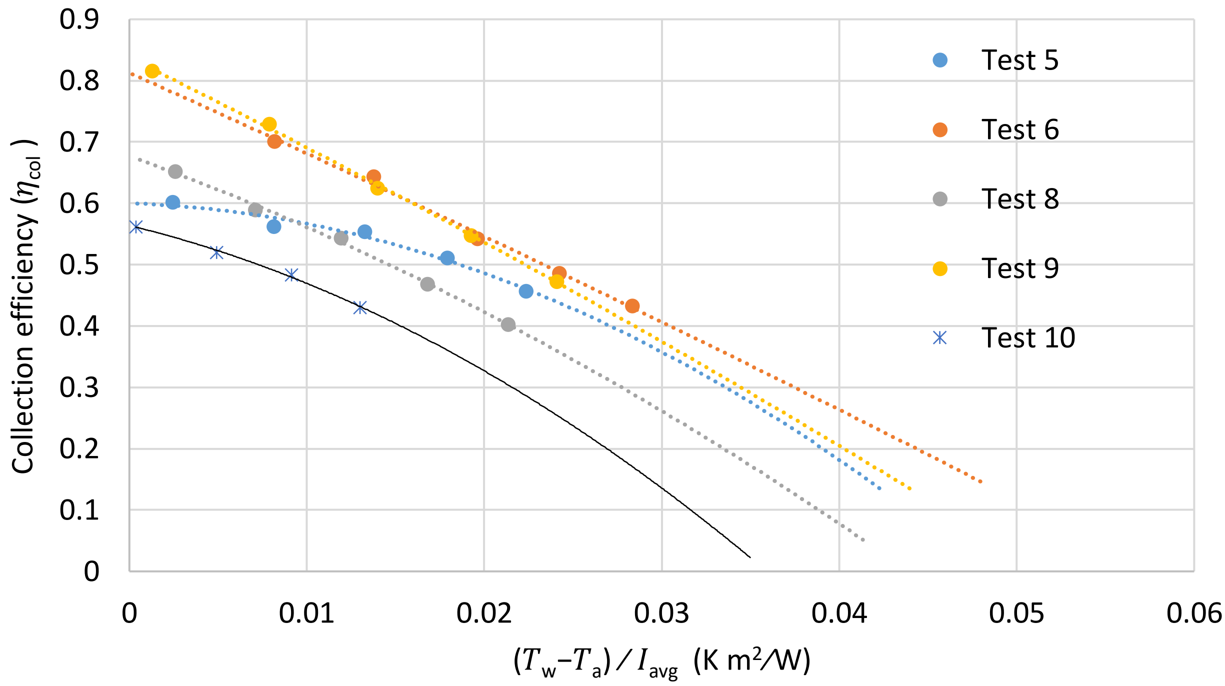

Figure 13. Nominal solar heating efficiency for various unit a2 ICSSWHs (under constant solar simulated radiation during the 6 hour collection period)

Tests 6 and 9 are identical bar the use of end cap insulation. Both variants exhibit superior collection efficiency curves, but the shallower gradient (F x U_L) observed in Test 6 indicates the importance of sufficient end cap insulation to improve conversion of captured heat to the store. Tests 6 and 8 are identical bar the use of the planar reflector. The difference is a consistent 12% points across the testing period, reinforcing the observation from the Table 2 test comparisons which indicated that the reflector could have an influence of between 2 and 9% on the daily collection efficiency. Tests 5 and 10 have no vacuum and the drop in collection performance is clear. The F(τα) values are much lower, due to the significant resistance to heat flow across the annulus without the phase change process. Again, the use of the reflector is seen to have a positive impact, even when no vacuum is applied.

Thermal retention performance

Concerning thermal losses $U_{sys}A_{ab}$ (W/K) during the overnight heat loss period, Equation 2 is used to estimate the coefficient of water storage thermal losses assuming an idealised exponential temperature decay.

$$U_{sys}A_{ab} = \left[\left(\rho C_{p,w} V_T\right)/\Delta t_N\right] \cdot \ln\left[\left(T_{i,N} - T_{a,N}\right)/\left(T_{f,N} - T_{a,N}\right)\right] \qquad (2)$$

where Δt_N refers to time interval of the considered heat loss period in seconds and $T_{a,N}$ the corresponding average ambient air temperature. Temperatures $T_{i,N}$ and $T_{f,N}$ are initial and final hot water temperatures during each interval of the cooling period respectively. The heat retention efficiency η_{ret} of the various units during the cooling period is shown in Equation 3.

$$\eta_{ret} = \left[\left(T_{f,N} - T_{a,N}\right)/\left(T_{i,N} - T_{a,N}\right)\right] \times 100 \qquad (3)$$

Combining Equations 2 and 3 can simplify $U_{sys}A_{ab}$ (W/K) to Equation 4

$$U_{\mathrm{sys}}A_{\mathrm{ab}} = \left[\left(\rho C_{\mathrm{p,w}}V_T\right)/\Delta t_{\mathrm{N}}\right] \cdot \ln[1/\eta_{\mathrm{ret}}] \quad (4)$$

Table 4 lists the heat loss characteristics for a range of the investigated ICSSWH prototypes. As stated by Pugsley et al [2020a] comparisons between heat loss coefficients must be made with caution because there is a lack of consistency concerning definitions for reference areas (such as the absorber, aperture, or whole envelope area) and because $U_{sys}A_{\mathrm{ab}}$ inherently increases in proportion to the physical size of the ICSSWH. To enable fair comparisons in relation to heat retention performance in ICSSWH units, Pugsley et al [2020a] proposed 2 new heat loss coefficient metrics, one of which is referenced to stored water volume ($U_{sys}A_{ab}/V$). Using this metric eliminates duration issues associated with η_{ret} and problems with comparing large volume units with small volume units, and those with strange aspect ratios.

Table 4: Heat loss characteristics for the investigated ICSSWH prototype

	Test	Heat retention efficiency (12 hrs) (η_{ret})	Heat retention efficiency (18 hrs) (η_{ret})	Heat loss coefficient U_{sys} (W/m^{2}K)	Heat loss coefficient $U_{sys}A_{ab}$ (W/K)	Heat loss coefficient $U_{sys}A_{ab}/V$ (W/m^{3}K)
a1. seam welded cone	No HTF, vacuum	0.57	0.44	1.58	1.42	55.17
	Low intensity	0.52	0.37	1.83	1.65	63.95
	Base case	0.51	0.35	1.90	1.71	66.20
	No reflector	0.53	0.38	1.78	1.56	60.47
a2. inset seam welded cone	No vacuum	0.52	0.39	1.73	1.53	63.18
	Base case	0.53	0.39	1.64	1.46	60.17
	No reflector	0.52	0.39	1.65	1.46	60.45
	No end insulation	0.45	0.31	2.04	1.81	74.75
	No vacuum No reflector	0.53	0.38	1.77	1.57	64.75
b. PVC cup insert	Base case	0.52	0.36	1.90	1.94	62.89
c. ABS hub with gasket	Insulated end caps	0.62	0.48	1.32	1.36	47.05
d. seam welded dish	No HTF film No cover	0.72	0.63	1.31	1.44	30.25
	No HTF film single cover	0.74	0.64	1.22	1.34	28.17
	No HTF	0.77	0.69	1.02	1.12	23.64

	film Double cover					
	Vertical Double cover	0.83	0.76	0.79	0.87	18.29
e. Acrylic hub with gasket	Base case	0.60	0.46	1.32	0.83	50.12

Overall unit d. seam welded dish exhibited the thermal heat retention efficiencies (η_{ret}) and corresponding system thermal loss coefficients. The unit d. tests shown in Table 4 are units without any HTF (but with vacuum). As seen previously, the lack of HTF seriously impedes the ability to collect absorbed solar radiation during the collection phase. During cooldown, however, the lack of vapour in the annulus reduces reverse mode transference. An added factor is the V/A_{ab} ratio as unit d has much higher ration compared to the other units studied. The evacuated, double vessel and bare absorber had a 12 hour thermal heat retention efficiency (η_{ret}) of 72% (63% 18 hours) ($U_{sys}A_{ab}/V$ = 30 W/m^{3}K), highlighting the potential performance that the thermal diode can achieve. Adding successful layers of transparent cover improves the retention yet further; single (η_{ret}) = 74% (64% 18 hours) ($U_{sys}A_{ab}/V$ = 28 W/m^{3}K), double (η_{ret}) = 77% (69% 18 hours) ($U_{sys}A_{ab}/V$ = 24 W/m^{3}K). Interestingly, mounting the unit vertically (whilst problematic in achieving a wetted film during collection) improves heat retention yet further at (η_{ret}) = 83% (76% 18 hours) ($U_{sys}A_{ab}/V$ = 18 W/m^{3}K). This was a characteristic observed in the vertical single glazed BIPV-PLVTD-ICSSWH reported by Pugsley et al [2020b] which had an 18 hour heat retention efficiency of 71% and $U_{sys}A_{ab}/V$ = 23 W/m^{3}K. The primary reason for the reduced heat loss is due to vessel stratification and the radiative view factor coupled with top end insulation.

The best horizontal unit, with lower V/A_{ab} ratios, was unit c. with (η_{ret}) of 62% over 12 hours (48% 18 hours) and heat loss coefficient referenced to stored water volume of $U_{sys}A_{ab}/V$ = 47 W/m^{3}K. A big factor in the retention performance was the low thermal conductance of the end caps (ABS). Units a1 and a2 have metal to metal welded end caps thus creating an unbroken direct conductive path from the inner vessel to the outer vessel, thus exacerbating heat loss during cool-down. Three tests highlight this thermal loss path perfectly; unit a1. base case, unit a2. base case, unit a2. with no end cap insulation. Comparing (η_{ret}) unit a1 = 51% (35% 18 hours) and $U_{sys}A_{ab}/V$ = 66 W/m^{3}K; unit a2 = 53% (39% 18 hours) and $U_{sys}A_{ab}/V$ = 60 W/m^{3}K; unit a2 (no end cap insulation) = 45% (31% 18 hours) and $U_{sys}A_{ab}/V$ = 75 W/m^{3}K. Unit a1 and unit a2 only differ with regards to the end welding configuration, a1. utilises a simple edge seam whilst a2. incorporates a more complex jointing design, to increase the length of conductive travel. However, this improvement is small when the impact of end insulation is considered. It is therefore very important to ensure that sufficient insulation (either end cap material or added) is used to reduce vessel end losses.

By way of comparison, Pugsley et al [2020a] state that averaged heat loss coefficient referenced to stored water volume taken from the body of material published in this area is $U_{sys}A_{ab}/V$ = 49 W/m^{3}K with the ideal being 10 W/m^{3}K. The horizontal cylindrical tank-in-tank, unit mounted in a two-part CPC reflector investigated by Souliotis et al [2017] had a $U_{sys}A_{ab}/V$ = 38 W/m^{3}K. Muhumuza et al [2019b] investigated the heat retention of several thermal diode ICSSWH units with different lengths and aluminium and stainless steel vessels. Values of $U_{sys}A_{ab}/V$ = 88 W/m^{3}K, 59 W/m^{3}K and 46 W/m^{3}K are presented for a 1m long aluminium unit, 1m long stainless steel unit and 1.6m long stainless steel unit, respectively.

Diode and overall performance

Diodicity is a dimensionless measure of thermal rectification and is a useful performance measure for thermal diodes. It is commonly defined as a scalar based on the apparent thermal conductivities (k) of the device in forward (f) heat transfer mode and reverse (r) insulation modes. Pugsley et al. [2019, 2020a] proposed and validated calculation methods and a parametric design approach for evaluating the thermal resistances exhibited by a PLVTD ICSSWH and developed a working prototype. Heat transfer through the PLVTD is driven by the difference in temperature between the two plates (evaporator (T_1) and condenser(T_2)). The transferred thermal power (q_{12}), the transferred heat flux (q_{12}/A_{ab}) and the overall thermal transmission (U_{fr}) through the PLVTD are related according to Equation 5.

$$U_{\text{fr}} = q_{12}/(A_{\text{ab}}\Delta T_{12}) \tag{5}$$

In forward mode, the dominant thermal transmission mechanism is latent heat transfer associated with working fluid liquid-vapour-liquid phase changes and the net transfer of working fluid vapour mass across the cavity between the two plates. In reverse mode, thermal transmission occurs via several different mechanisms including working fluid convection and gaseous conduction; radiation between the plates; and conduction through the external envelope and end supporting structural elements.

Table 5: Overall thermal transmission in forward (f) heat transfer mode and reverse (r) insulation modes for selected welded ICSSWH prototypes

	Test	U_f (W/m^{2}K)	U_r (W/m^{2}K)	24 hour diurnal efficiency ($\eta_{\text{col 24}}$)
a1. seam welded cone	No HTF, vacuum	6.30	2.26	0.12
	Low intensity	20.56	2.58	0.16
	Base case	23.96	2.62	0.17
	No reflector	19.59	2.66	0.15
a2. inset seam welded cone	No vacuum	18.17	2.43	0.21
	Base case	36.11	2.00	0.22
	No reflector	31.41	2.00	0.21
	No end insulation	35.43	2.45	-
	No vacuum, no reflector	21.42	2.86	0.19
d. seam welded dish	No HTF film, no cover	4.42	1.47	0.12
	No HTF film, single cover	4.09	2.22	0.12
	No HTF film, double cover	4.60	1.98	0.13

The thermal transmission in both the forward heat transfer and reverse insulation modes shown in Table 5, broadly mirror the results observed in collection and heat retention efficiencies. Unit a2, the inset seam welded cone design with optimal operating features had the best diurnal thermal ($\eta_{\text{col 24}}$) efficiency (product of the collection and retention efficiencies over the 24 hour period) at 22% as expected given the high forward heat transfer (36.1 W/m^{2}K) and low reverse insulation mode (2.0 W/m^{2}K). Unit d, the seam welded dish design (all presented forms), highlights the importance of the HTF in the forward mode. At around 4 W/m^{2}K, it exhibits the lowest forward mode heat transfer value, resulting in a low collection efficiency (see Table 2). The lack of HTF, however marginally improves (or rather reduces) heat flow in the reverse mode, having the lowest observed value (1.47 W/m^{2}K) of any of the units tested, although there is some deviation when covers are introduced. It is not entirely clear why this is, but it is assumed to be due to the very low tank temperatures and their influence by small changes in the ambient during cooldown and influence of kinematic viscosity in the gas in the annulus. The collective diurnal thermal efficiency ($\eta_{\mathrm{col}\,24}$) for all 3 versions of unit d, with no HTF is very low at 12 to 13%. From studies on vertical, pumped film units (based on unit design d) cold-start daily collection efficiencies and 18 hour heat retention efficiencies of 52% (table 2) and 76% (table 4), respectively are achievable, giving an effective diurnal thermal ($\eta_{\mathrm{col}\,24}$) efficiency of 39%. Clearly, there is more that can be done to improve the overall performance of the the passive horizontal units investigated in this study and it is this goal that drives the authors in the continued work in this area.

6.0 CONCLUSION

Integrated Collector Storage Solar Water Heaters (ICSSWH) are simple, low cost solar devices. ICSSWHs have developed significantly and they have the potential to broaden the scope of current small-scale solar hot water systems for single and multi-family dwellings, particularly in warm climates. Their continual development and improvement as simple, reliable and low-cost configurations is essential to achieve increased interest in the general solar heat market globally. Many recent studies have focused on the improvement of the thermal performance of ICSSWH systems through the development of the thermal diode ICSSWH based on a double vessel concept.

This paper presents for the first time a systematic evaluation of horizontal ICSSWH prototypes developed at the Centre for Sustainable Technologies (CST) at Ulster University. The study introduces the use the novel, patented double vessel, thermal diode feature (to enhance heat retention during non-collection periods) within a range of horizontal unit configurations that have evolved from the initial investigations around liquid-vapour phase change materials (PCM) and very low annulus cavity pressures in ICSSWHs. The energy performance evaluation and characterisation of different prototype designs under solar simulated experimental conditions has been conducted and the subsequent parametric analysis presented.

A balance between performance and physical/operational considerations is thus necessary. Careful design of the components and configuration, best selection and use of materials, optimal metrics, such as the volume/area ratio and designs tailored to meet climatic, aesthetic, infrastructural and economic operational conditions should always be adhered to. This work demonstrates that new and innovative design solutions that are readily achievable (in materials, fabrication and assembly) can be formulated to improve the performance of simple double-vessel cylindrical ICSSWHs. The work highlights the importance of augmenting heat transfer across the annulus cavity and demonstrates the improvement of the cold-start daily collection efficiency from around (η_{col}) of 20% (no HTF), to around 50% (with HTF but no vacuum), and >55% when the annulus is evacuated to remove non-consensable gases and form a liquid-vapour phase change thermal diode. Annulus thermal diode heat transfer coefficients of around (U_{fr}) 35 W/m^{2}K in forward mode and 2W/m^{2}K in reverse mode have been demonstrated. Lower annulus heat transfer coefficients (1.5W/m^{2}K) are achievable when there is no HTF in the annulus, but the relatively modest improvement in overnight heat retention performance achieved is negligible when compared to the dramatic loss of solar collection efficiency. This is clearly apparent when comparing diurnal thermal efficiencies which are typically limited to around ($\eta_{\mathrm{col}\,24}$) 12% when there is no HTF but can reach 22% when HTF and annulus vacuum are implemented.

The importance of insulating the ends of the vessels has also been demonstrated with uninsulated ends typically introducing significant overnight heat losses. Heat retention performances of ($U_{sys}A_{ab}/V$) 60 W/m^{3}K (12 hour heat retention of 53%) are achievable when end caps are insulated but performances are limited to 75 W/m^{3}K (12 hour heat retention of 45%) if the ICSSWH has uninsulated metal ends. Increasing the conductive path lengths between outer and inner vessels has been shown to increase both solar collection and heat retention efficiencies significantly, improving diurnal thermal efficiency from ($\eta_{col\,24}$) 17% in the case of a conventional metal end cap to 22% when a novel inset welded design was employed.

Common to most solar thermal collectors, provision of one or more transparent covers are required to reduce absorber heat loss, although optical losses need to be considered, especially when double-cover solutions are proposed. Augmenting a thermal diode double-vessel cylindrical ICSSWHs using a simple, low cost, planar reflector has been shown to be very effective, increasing collection efficiencies by up to 12%. The best collection efficiency achieved for a thermal diode double-vessel cylindrical ICSSWH with single transparent cover, planar reflector, insulated inset welded metal end caps (prototype a2.) was (η_{col}) 57%. A similar unit but with plastic end caps (prototype c.) achieved (η_{col}) 61%. Corresponding operational collection efficiencies at $(T_w\text{-}T_a)\,/\,I_{ave} \approx 0.035 m^2K/W$ were found to be ($\eta_{col(0.035)}$) 34 and 35% respectively, similar to many of the best double-vessel cylindrical ICSSWHs reported in the literature but without requiring a complicated, bulky, and expensive parabolic reflector. Corresponding overnight heat retention coefficients achieved by prototypes a2. and c. were $U_{sys}A_{ab}/V$ = 60 W/m^{3}K. (18 hour heat retention of 39%) and $U_{sys}A_{ab}/V$ = 47 W/m^{3}K (18 hour heat retention of 48%) respectively, which is better than most devices reported in the literature.

Overall, this study has shown that design enhancements such as inset welded design end caps, transparent covers, targeted insulation, end cap combined sealing and mounting assembly, integrated into an already innovative thermal diode operating concept can provide a solar water heating system that has a relatively good (comparative) performance. The optimised prototype to be developed from this study for subsequent field trials will use the fully hermetically sealed, metal to metal welded inset cap end configuration, with optimised HTF and vacuum capacities, using tailored end cap insulation and reflector elements. This design can deliver a 24 hour diurnal efficiency ($\eta_{(col\ 24)}$) of 22% (84% greater than the base case welded unit) but still presents a simple, mass manufacturable design in both materials and components, requiring no parasitic pumping or control power to operate, still easy to install and connect but crucially offers the potential for much lower costs and therefore more cost-effective hot water for many in the developing world.

Acknowledgments
The work presented in this paper was supported by SolaForm Ltd, the “SolaFin2Go” and “SolaNetwork” projects funded by the UKRI Engineering and Physical Sciences Research Council. The authors would also like to thank networking support funded by the European Union ERASMUS programme.

Nomenclature

A_{ab}	absorber area (m^2)
A_{ap}	collector area (m^2)
$C_{p,w}$	specific heat capacity of water at constant pressure ($J\,kg^{-1}K^{-1}$)
F	heat removal factor
I_{avg}	constant average light intensity (W/m^2)
m_w	mass of water in the inner storage vessel (kg)
q_{12}	transferred thermal power (W)
Q_{col}	thermal energy collected (J)
Q_{ap}	total energy incident on the aperture (J)
$T_{w,i}$	average initial temperature of the stored water (°C)
$T_{w,f}$	average final temperature of the stored water (°C)
T_w	average water temperature (°C)
T_a	average ambient air temperature (°C)

$T_{a,N}$ average ambient air temperature of the time interval (°C)
$T_{i,N}$ final hot water temperature (°C)
$T_{f,N}$ final hot water temperature (°C)
$(T_w-T_a)/I_{ave}$ solar thermal condition (Km^2/W)
U_{sys} system thermal loss coefficient (W/m^2K)
$U_{sys}A_{ab}$ heat loss coefficient per area of absorber (W/K)
U_{fr} overall thermal transmission (W/m^2K)
U_f thermal transmission in the forward (collection) mode (W/m^2K)
U_r thermal transmission in the reverse (retention) mode (W/m^2K)
(V/A_{ab}) volume-to-absorber area ratios (m^3/m^2)
V or V_T inner vessel storage volume (m^3)

Greek
Δt collection period (seconds)
Δt_N time interval of the considered heat loss period (seconds)
ρ water density (kg/m^3)
η_{col} mean collection efficiency
η_{ret} thermal heat retention efficiency
η_T instantaneous solar thermal collection efficiency
$\eta_{col(0.035)}$ operational collection efficiency
$\eta_{col\ 24}$ diurnal thermal efficiency
$(\tau\alpha)$ transmittance- absorptance product

References

G. Amerongen, J. Lee, J. Suter (2013) Legionella and solar water heaters. Report commissioned by the Solar Certification Fund. Available at: <www.estif.org/solarkeymarknew/images/downloads/SCF/scfdeliverables/Report%20SCF%20Legionella%20and%20 solar%20water%20heaters%20%20Final%202013%2004.pdf>

E.Aranovitch, D.Gilliaert, W. B.Gillett and J.E. Bates (1986) Test methods for solar water heating systems. In Proceed ings of 5th meeting of European Solar Collector and Systems Group, Seville, Spain, pp. 149–194.

J.B. Boreyko, Y. Zhao, C.-H. Chen (2011) Planar jumping-drop thermal diodes, Applied Physics Letters. 99

J.B. Boreyko, C.-H. Chen (2013) Vapor chambers with jumping-drop liquid return from superhydrophobic condensers, International Journal Heat Mass Transfer. 61 pp 409–418

British Standards Institution (2013) BS ISO 9459-4:2013, Solar heating. Domestic water heating systems. System performance characterization by means of component tests and computer simulation.

K. Butti, J. Perlin (1981) A Golden Thread, Marion Boyars Publishers Ltd., London, UK

H.A. De Beijer (1998) Product development in solar water heating, in: Proceedings of the 5th World Renewable Energy Congress, Florence, Italy, 1998, pp. 201 – 204.

D. Faiman (1984) Towards a standard method for determining the efficiency of integrated collector–storage solar water heaters. Solar Energy 33, pp 459–463

H. Jouhara, A. Chauhan, T. Nannou, S. Almahmoud, B. Delpech, L.C. Wrobel (2017) Heat pipe based systems - Advances and applications. Energy. 128, pp. 729-754

S. Kalogirou et al (2017) Building Integrated Solar Thermal Systems, Design and Applications Handbook. COST Action TU1205. COST Office, ISBN: 978-9963-697-22-9

C. Lamnatou, M. Smyth, D. Chemisana (2019) Building-Integrated Photovoltaic/Thermal (BIPVT): LCA of a façade-integrated prototype and issues about human health, ecosystems, resources. Science of the Total Environment, 660, pp 1576-1592

J.D. Mondol, V.V.N. Kishore, M. Smyth, A. Zacharopoulos, A. Kansal, M. Anderson (2013) Solar Accelerator Anerobic Digester Design for Small-scale Bio-gas Production. Conference Proceeding, 21st European Biomass Conference and Exhibition, Copenhagen, Denmark, July 2013 pp 1233-1238

R. Muhumuza, A. Zacharopoulos, J.D. Mondol, M. Smyth, A. Pugsley, G. (2019a) Experimental study of heat retention performance of thermal diode Integrated Collector Storage Solar Water Heater (ICSSWH) configurations. Sustainable Energy Technologies and Assessments, 34, pp 214-219

R. Muhumuza, A. Zacharopoulos, J.D. Mondol, M. Smyth, A. Pugsley, G. FrancescoGiuzio, D. Kurmis (2019b). Experimental investigation of horizontally operating thermal diode solar water heaters with differing absorber materials under simulated conditions. Renewable Energy, 138, 1051-1064.

R. Muhumuza (2020) Solar Cogeneration for Access to Energy in Off-grid Rural Households in Developing Countries (DCs). (PhD Thesis), University of Ulster, UK, 2020.

A. Pugsley, M. Smyth, J.D. Mondol, A. Zacharopoulos, L.D. Mattia (2016) Experimental characterisation of a flat panel integrated collector-storage solar water heater featuring a photovoltaic absorber and a planar liquid-vapour thermal diode. Conference Proceeding, EuroSun, Palma de Mallorca, Spain. October 2016

A. Pugsley, M. Smyth, J.D. Mondol, A. Zacharopoulos (2019) Theoretical and experimental analysis of a horizontal planar Liquid-Vapour Thermal Diode (PLVTD). International Journal of Heat and Mass Transfer, 144, pp 1-34

A. Pugsley, M. Smyth, J.D. Mondol, A. Zacharopoulos (2020a) BIPV/T facades – a new opportunity for Integrated Collector Storage Solar Water Heaters? Part 1: State-of-the-art, theory and potential. In press.

A. Pugsley, M. Smyth, J.D. Mondol, A. Zacharopoulos (2020b) BIPV/T facades – a new opportunity for Integrated Collector Storage Solar Water Heaters? Part 2: Physical realization and laboratory testing. In press

P. Quinlan (2010) The Development of a Novel Integrated Collector Storage Solar Water Heater (ICSSWH) Using Phase Change Materials and Partial Evacuation (PhD Thesis), University of Ulster, UK, 2010.

C. Schmidt, A. Goetzberger (1990) Single-Tube Integrated Collector Storage Systems with Transparent Insulation and Involute Reflector. Solar Energy 45 (2) pp 93-100

R. Singh, I.J. Lazarus, M. Souliotis (2016) Recent developments in integrated collector storage (ICS) solar water heaters: a review, Renewable Sustainable Energy Review. 54 pp 270 – 298.

A. Shafieian, M. Khiadani, A.Nosrati (2018) A review of latest developments, progress, and applications of heat pipe solar collectors. Renewable and Sustainable Energy Reviews 95, pp. 273-304

M. Smyth, P.C. Eames, B. Norton (2006) Integrated collector storage solar water heaters, Renewable Sustainable Energy Review. 10 (6) pp 503 - 538.

M. Smyth, P. Quinlan, J.D. Mondol, A. Zacharopoulos, D. McLarnon, A. Pugsley (2017a) The evolutionary thermal performance and development of a novel thermal diode pre-heat solar water heater under simulated heat flux conditions, Renewable Energy. 113 pp 1160–1167.

M. Smyth, A. Pugsley, G. Hanna, A. Zacharopoulos, J.D. Mondol, A. Besheer (2017b) Experimental performance comparison of a Hybrid Photovoltaic/Solar Thermal (HyPV/T) Façade Module with a flat ICSSWH module. First International Conference on Building Integrated Renewable Energy Systems, BIRES 2017, Dublin, Ireland, March 2017

M. Smyth, P. Quinlan, J.D. Mondol, A. Zacharopoulos, D. McLarnon, A. Pugsley (2018) The experimental evaluation and improvements of a novel thermal diode pre-heat solar water heater under simulated solar conditions, Renewable Energy. 121 pp 116–122.

M. Smyth, G. Barone, A., Buonomano, C. Forzano, G.F. Giuzio, A. Palombo, J.D. Mondol, R. Muhumuza, A. Pugsley, A. Zacharopoulos, D. McLarnon. (2019a) A novel Integrated Collector

Storage Solar Water Heating (ICSSWH) prototype: experimental investigation and simulation model. Conference Proceeding, SDEWES 2019 - 14th Conference on Sustainable Development of Energy, Water and Environment Systems, Dubrovnik, Croatia, October 2019.

M. Smyth, J.D. Mondol, A. Pugsley, A. Zacharopoulos, A. Besheer (2019b) Experimental performance characterisation of a Hybrid Photovoltaic/Solar Thermal Façade module compared to a flat Integrated Collector Storage Solar Water Heater module, Renewable Energy. 137, pp 137-143

M. Smyth, G. Barone, A., Buonomano, C. Forzano, G.F. Giuzio, A. Palombo, J.D. Mondol, R. Muhumuza, A. Pugsley, A. Zacharopoulos, D. McLarnon. (2020) Modelling and experimental evaluation of an innovative Integrated Collector Storage Solar Water Heating (ICSSWH) prototype. Renewable energy. In press. Available online 18 May 2020

Solaform, 2014. http://solaform.com.

"A solar water heater" - International Publication number WO 2010/052010 A2, "

M. Souliotis, P. Quinlan, M. Smyth, Y. Tripanagnostopoulos, A. Zacharopoulos, M. Ramirez, P. Yianoulis (2011) Heat retaining integrated collector storage solar water heater with asymmetric CPC reflector, Solar Energy 85 (10) pp 2474 - 2487.

M.Souliotis, S. Papaefthimiou, Y.G. Caouris, A. Zacharopoulos, P. Quinlan, M. Smyth (2017) Integrated collector storage solar water heater under partial vacuum. Energy, 139 pp 991-1002

US department of energy, Weather Data, EnergyPlus, (n.d.). https://energyplus.net/weather (accessed march, 2019).

Y. Tripanagnostopoulos, M. Souliotis and T.H. Nousia (2002) CPC Type Integrated Collector Storage Systems. Solar Energy Vol. 72, No. 4, pp. 327–350, 2002

A. Zacharopoulos, J.D. Mondol, M. Smyth, T. Hyde, V. O’Brien (2009) State-of-the-art solar simulator with dimming control and flexible mounting, in: Proceedings ISES Solar World Congress. 2009 Renewable Energy Shaping Our Future. 11-14 Oct., International Solar Energy Society, Johannesburg, South Africa, 2009: p 854.